A Numerical Study for Blow-up in Solutions of the Generalized 2-D Benjamin-Ono Equation

Farida Bousbia and Fatma Zohra Nouri

***Abstract*—The Benjamin-Ono (BO) equation is a nonlinear partial integro-differential equation that describes internal waves in deep stratified fluids. Here we present a numerical study of the blow-up phenomenon for the BO-generalized KP version with different types of nonlinearities. A dynamic rescaling is used to identify the type of the singularity and explore the investigation of observed blow-ups. For the numerical experimentations, an exponential time-differencing fourth-order Runge-Kutta method combined with a space-scheme based on the Fourier spectral method is used.**

***Index Terms*—Benjamin-Ono equation; Spectral Methods.**

I. Introduction

Water waves are dispersive, i.e. have longer wavelengths and travel faster. Dispersion can arise from the constraints or bound nature, of the particle component in a given medium. For example, the following equations are models for water waves in interesting physical settings:

1- The nonlinear Shrödinger flow is the universal model for dispersive waves in 1-d with nondegenerate dispersion, valid in a small frequency window and at small amplitudes.

2- The Korteweg-de Vries (1895) flow describes the evolution of unidirectional waves of small amplitude and long wavelength in shallow water, for more details see [13].

3- The Benjamin-Ono flow was introduced by Benjamin (1967) and Ono (1975), as a model for the propagation of one dimensional internal waves in deep water, i.e. wave propagation at the interface of layers of fluids with different densities. More recently, it was derived as a model for small amplitude and long wavelength in constant vorticity flows.

These partial differential equations (PDEs) have common features, such as they are completely integrable, globally well-posed with an infinity conservation laws and admit soliton solutions.

This paper is organized as follows. The next section is devoted to a study of some known linear dispersive equations, followed by two sections on the KP-BO equations and their dynamic rescaling. In Section 5, we set the numerical discretisations, revealing first the L_2 critical case, then the blow-up cases, followed by an extention to the supercritical case. Finally numerical results with comments and concluding remarks are presented.

Manuscript received May 21, 2019; revised September 8, 2019. This work was supported in part by the MERS-Algerian Phd Grant.

F. Bousbia[1] and F.Z. Nouri[2] are with the Mathematical Modeling and Numerical Simulation Laboratory, Faculty of Sciences, Badji Mokhtar University, P.O. Box 12, Annaba-ALGERIA, e-mail: [1]bousbia@hotmail.com,[2]tassili.nan09@gmail.com

II. Some linear dispervive equations

Let us consider the following dispersive wave equations

$$u_{tt} = u_{xx} - u(KG), u_t = u_{xxx}(KDV), u_t = H(u_{xxx})(BO),$$

$$u_t = iu_{xx}(S),\ u_t\ - u_x = u_{xxt}(RLW).\ \textbf{(*)}$$

These PDEs are respectively known as the Klein-Gordon (KG), Korteweg-de Vries (KDV), Benjamin-Ono (BO), Shrödinger (S) and the regularised long wave (RLW) equations, where for the case of (BO), H is the Hilbert transform on the real line. If we write $u(x,t) = \exp(i(kx - wt))$, their corresponding dispersion relations are respectively given by

$$w^2 = k^2 + 1, w = k^3, w = sign(k)k^2, w = k^2, w = k/(1+k^2)$$

and they enable one to solve these PDEs, analytically involving Fourier integrals, and numerically by computing them with the discrete fast Fourier transform FFT. Note that these dispersion relations, and particularly $\frac{dw}{dk}$ give a complete description of the evolution of each wave equation.

A. Fourier Spectral Approach

For the numerical Fourier spectral-based approximations, one proceeds as follows: a given initial condition is converted to Fourier space via the FFT to give the coefficients $a(k,0)$. Then the solution is advanced in Fourier space with respect to the time variable t to get $a(k,t) = a(k,0)\exp(-iw(k)t$. An inverse FFT brings us back to $u(x,t)$. The errors incurred here are those in approximating the Fourier integrals with the FFT. These errors can be rendered small by taking many points in the FFT and choosing a sufficiently large space interval so that the waves do not touch the boundaries, particularly for a problem with a strong dispersion.
Here we plot the solution of the five PDEs **(*)** with the same initial condition, on the same space interval. The solutions are plotted at different times t, for example for a PDE with a strong dispersion, such as the (KDV), we could go only to about $t = 1$ before the waves reached the edge of the computational domain; while for weak dispersion cases such as the (KG) and (RLW), we could go up to $t = 10$ or $t = 20$ for $u(x,0) = \cos(x), x \in [-20, 20]$; and to $t = 20$ or $t = 25$ for $u(x,0) = sech(x), x \in [-40, 40]$ (see Fig. 1.).
Inspired by these results, we are interested to study the dispersive decay of long time solutions for small localized data and explore the blow-up phenomenon of the generalized BO-equation with different types of nonlinearities.

III. Generalised Benjamin-Ono equation

Recently, the study of the generalization of the BO equation for weak transverse perturbations has become more meaningful for researchers in many fields. To our Knowledge, there is no class of $(1+2)$-dimensional BO equations

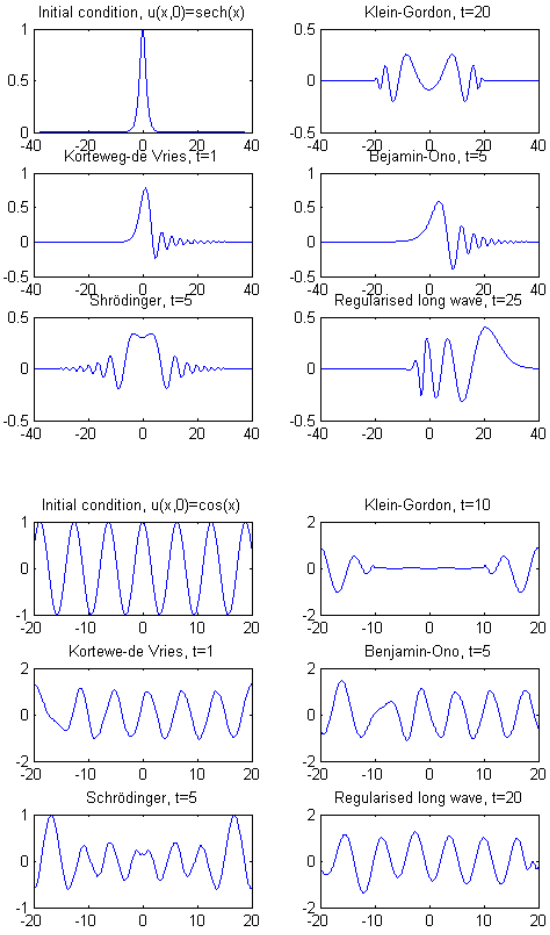

Fig. 1. Numerical wave evolution of equations (*):
Top for $u(x,0) = sech(x)$, and bottom for $u(x,0) = cos(x)$.

known to be integrable. However, there are some interesting results concerning a larger class of these equations, see [4], [11] and [16] for a more recent review.
The KP-BO equations describe the motion of long, weakly nonlinear internal waves in a deep stratified fluid with weak transverse effects (see [5] for more details). By using different techniques, these equations have been studied by several authors, for example:

- In [3], the authors have developed a proof for the solution's local well-posedness by the use of a method due to Kato [7], and investigated its blows-up in finite time, for suitable conditions as in [15].
- Esfahani has claimed in [2] the existence of solitary waves, by a suitable application of the anisotropic Sobolev embedding theorem.
- More recently, by the use of the so-called minimax theory techniques and the Lizorkin's theorem. The existence, regularity and analyticity properties of their solitary waves, were established in [16] .
- For the case when $p = 1$, some interesting results were shown, such as analytical stability issues for (1) can be found in [5], the existence of global solutions and scattering was proved for small, smooth and localized initial data (see [4]) and the local Cauchy problem of the gKP-BO was studied in [11].

In the following we focus on a class of the generalized two dimensional BO equations (GKP-BO) written as:

$$(u_t - \mathrm{H}u_{xx} + u^p u_x)_x = \lambda u_{yy}, \quad \lambda = \pm 1, \tag{1}$$

or in the integrated form as

$$u_t - \mathrm{H}u_{xx} + u^p u_x = \lambda \partial_x^{-1} u_{yy}, \quad \lambda = \pm 1, \tag{2}$$

with $p = \frac{n_1}{n_2}$, n_1, $n_2 \in N^*$ and $\lambda = 1$ in the case of (GKPI-BO) or $\lambda = -1$ for (GKPII-BO). The operator H is the Hilbert transform operator defined by

$$\mathrm{H}u(x,y,t) = \frac{1}{\pi} P.V. \int_R \frac{u(z,y,t)}{z-x} dz. \tag{3}$$

$P.V.$ stands for the principal value.
Here ∂_x^{-1} is defined via the Fourier transform by

$$\widehat{\partial_x^{-1} f}(k_x, k_y) = \frac{1}{\mathrm{i}k_x} \widehat{f}(k_x, k_y). \tag{4}$$

Equations (2) satisfy some conservation quantities such as the *mass*, given by the L_2 norm of u as

$$M[u] = \|u\|_2, \tag{5}$$

and the *energy* by

$$E[u] = \int_{R^2} [-\tfrac{1}{2} u_x H u - \tfrac{1}{(p+1)(p+2)} u^{p+2} + \frac{\lambda}{2} (\partial_x^{-1} u_y)] \, dxdy. \tag{6}$$

In addition they have localized travelling wave solutions in the x-direction of the form $u(x;y;t) = Q(x-ct;y)$, where the nontrivial $Q(z;y)$ satisfies

$$-cQ_{zz} + \frac{1}{n+1} Q_{zz}^{p+1} - HQ_{zzz} - \lambda Q_{yy} = 0. \tag{7}$$

Due to the antiderivative term $\partial_x^{-1} u_{yy}$ in (2), $\forall t > 0$ the solutions satisfy the constraint

$$\int_R u_{yy} dx = 0. \tag{8}$$

Furthermore a singularity at the x frequency $k_x = 0$ delimits the achievable precision in the solutions of the GKP-BO equations. It was proved that the solutions to a Cauchy problem will not be smooth in time for $t = 0$ if they do not satisfy the constraint (8). Numerically it was reported in [10] that the solutions develop an infnite trench. This non-regularity represented numerically when $t \to 0$, presents a problem as it delimits the manageable accuracy. To avoid such problems, we consider initial data that are x-derivatives of rapidly decreasing functions satisfying (8). In this paper, we consider the following initial data

$$u_0(x,y) = \beta \exp(-(x^2+y^2)), \beta \text{ is a constant}. \tag{9}$$

IV. Dynamic Rescaling

Equation (2) is symmetric under the following rescaling

$$\xi = \frac{x - x_m}{L}, \quad \eta = \frac{y - y_m}{L^{\frac{3}{2}}}, \quad \frac{d\tau}{dt} = \frac{1}{L^2}, \quad U = L^{\frac{1}{p}} u. \tag{10}$$

with a dynamic rescaling $L = L(t)$. Hence we write (2) as

$$U_\tau - a\left(\tfrac{1}{p}U + \xi U_\xi + \tfrac{3}{2}\eta U_\eta\right) - v_\xi U_\xi - v_\eta U_\eta + U^p U_\xi -$$

$$HU_{\xi\xi} = \lambda \int_{-\infty}^{\xi} U_{\eta\eta} dz, \tag{11}$$

with

$$a = \frac{L_\tau}{L}, v_\xi = \frac{x_{m,\tau}}{L} \; and \; v_\eta = \frac{y_{m,\tau}}{L}, \tag{12}$$

where x_m, y_m are the locations of the minimum or the maximum and the index τ denotes the τ-derivative.
Equation (11) can describe an asymptotic blow-up. It is expected that when $\tau \to \infty$, the functions U, v_η, v_ξ and a become independent of τ (can be denoted by an upperscript ∞), so that (11) becomes

$$U_\tau^\infty - a^\infty\left(\tfrac{1}{p}U^\infty + \xi {U_\xi}^\infty + \tfrac{3}{2}\eta {U_\eta}^\infty\right) - v_\xi^\infty U_\xi^\infty -$$

$$v_\eta^\infty U_\eta^\infty + (U^\infty)^p {U_\xi}^\infty - HU_{\xi\xi}^\infty = \lambda \int_{-\infty}^{\xi} U_{\eta\eta}^\infty dz. \tag{13}$$

In this case, there are two different scenarios, either an algebraic or an exponential decay of the scaling factor $L(\tau)$.

In the algebraic case, we have $L(\tau) = C_1\tau^{\gamma_1}$ with a constant C_1. Thus $\gamma_1 < -\frac{1}{2}$ and $a^\infty = 0$ give

$$L(t) \propto (t^* - t)^{\frac{1}{2+\frac{1}{\gamma_1}}}, \tag{14}$$

where t^* is the blow-up time. Then for $v_\eta^\infty = 0$, (13) reduces to an equation for the travelling wave solutions of the GKP-BO type, in a moving frame which has a unique nontrivial localized solution (7). Note that the constraint (8) is automatically satisfied for inivial data with a symmetry with respect to y or $-y$. Since the GKP-BO equation is invariant under (10), we have $v_\eta^\infty = 0$.

For an exponential decay, we have $L(\tau) = C_2 \exp a^\infty$ with $C_2 = const$ and $a^\infty < 0$, such that (11) implies

$$L(t) \propto (t^* - t)^{\frac{1}{2}} \tag{15}$$

For the numerical implementation, L, v_ξ and v_η have to be chosen in a convenient way. A possible choice is to assume that the single global minimum of U to be $U_\eta^0 = U_\xi^0 = 0$, for $\xi = \eta = 0$. This implies

$$\begin{pmatrix} U_{\xi\xi}^0 & U_{\xi\eta}^0 \\ U_{\xi\eta}^0 & U_{\eta\eta}^0 \end{pmatrix} \begin{pmatrix} v_\xi \\ v_\eta \end{pmatrix} = \begin{pmatrix} (U^0)^p U_{\xi\xi}^0 - HU_{\xi\xi}^0 + \lambda U_{\eta\eta}^0 \\ (U^0)^p U_{\xi\eta}^0 - HU_{\xi\xi\eta}^0 + \lambda U_{\eta\eta\eta}^0 \end{pmatrix}. \tag{16}$$

The coordinate transformation (10) yields

$$\| u \|_2^2 = L^{\frac{-2}{p}+\frac{5}{2}} \| U \|_2^2 . \tag{17}$$

Thus the L_2 critical case is $p = \frac{4}{5}$ and we get

$$\| u_x \|_2^2 = L^{\frac{1}{2}-\frac{2}{p}} \| U_\xi \|_2^2, \tag{18}$$

which implies the invariance under (10) for $p = 4/5$. Since the blow-ups in [3] are established for $\| u_y \|_2^2$, we consider

$$\| u_y \|_2^2 = L^{-(\frac{1}{2}+\frac{2}{p})} \| U_\eta \|_2^2 . \tag{19}$$

By fixing $||U_\eta||$ to be constant, we get

$$a = \frac{2p}{(2+p)(1+p)\|U_\eta\|} \int_{R^2} U^{p+1} U_{\eta\eta\xi} d\xi d\eta. \tag{20}$$

This will be chosen for the numerical implementation. The quantity $L(\tau)$ and the physical time t can be computed by the trapezoidal rule. The accuracy of the numerical solution is controlled by (17) and the energy by

$$E[u] = \frac{1}{L^{\frac{2}{p}-\frac{3}{2}}} \int_{R^2} [-\tfrac{1}{2} U_\xi H U - \frac{1}{(p+1)(p+2)} U^{p+2} +$$

$$\frac{\lambda}{2}(\partial_\xi^{-1} U_\eta)] d\xi d\eta. \tag{21}$$

Note that the energy is invariant under the rescaling (10) and the case $p = \frac{4}{3}$ is energy critical.

V. Numerical discretisation

In this section, the GKP-BO equations (2) is numerically discretised. Due to the periodicity, the Fourier spectral methods are the most convenient approaches for space-variable approximations, we refer to [1] and [12] for more details on these methods. For the integration of the resulting semi discrete stiff systems, a fourth order exponential time differencing (ETD) scheme is applied.
The 2d Fourier transform is defined by:

$$\hat{u}(k_x, k_y) = \int_{-\infty}^{\infty}\int_{-\infty}^{\infty} e^{-i(k_x x + k_y y)} u(x, y) dx dy. \tag{22}$$

Equation (2) is equivalent in Fourier space to

$$\hat{u}_t = \mathrm{N}(\hat{u}) + \mathrm{M}\hat{u}, \tag{23}$$

where $\mathrm{N}(\hat{u}) = -\mathrm{i}k_x \widehat{\frac{u^{p+1}}{p+1}}$, and $\mathrm{M} = -\mathrm{i}\,\mathrm{sgn}(k_x)k_x^2 + \lambda\frac{\mathrm{i}k_y^2}{k_x}$. For the numerical approximation of (23), we use a discrete Fourier transform that will be computed by a FFT. For the time integration, it was shown in [9] and [14] that the ETD schemes are most efficient for the KP-BO equations (see [6]). Here we use a modified version of these methods, namely the *exponential time-differencing fourth order Runge Kutta* (ETDRK4) scheme, which is suited for stiff systems. This explicit method is very appropriate as it can avoid a pollution of the Fourier coefficients and allows us to use small time steps to maintain the numerical stability.

The ETDRK4 schemes are based on ETD methods combined with the fourth-order Runge–Kutta time-stepping. The basic idea in the ETD is to integrate (23) exactly over a time step of length h with respect to t. If we write $\widehat{u}(t_n) = \widehat{u}_n$, and $\widehat{u}(t_{n+1}) = \widehat{u}_{n+1}$, then we get

$$\widehat{u}_{n+1} = e^{Mh}\widehat{u}_n + \int_0^h e^{M(h-\sigma)} N(\widehat{u}(t_n + \sigma), t_n + \sigma) d\sigma.$$

Hence the ETDRK4 schemes are given as follows: if we set

$$\begin{aligned}
a_n &= \widehat{u}_n E_2 + (E_2 - I)N(\widehat{u}_n, t_n)M^{-1}, \\
b_n &= \widehat{u}_n E_2 + (E_2 - I)N(a_n, t_n + h/2)M^{-1}, \\
c_n &= \widehat{a}_n E_2 + (E_2 - I)(2N(b_n, t_n + \frac{h}{2}) - N(\widehat{u}_n, t_n))M^{-1}, \\
\phi_1 &= (M^2h^2 - 3Mh + 4)E_1 - Mh - 4, \\
\phi_2 &= (Mh - 2)E_1 + Mh + 2, \\
\phi_3 &= (-Mh + 4)E_1 - M^2h^2 - 3Mh - 4;
\end{aligned}$$

so that

$$\begin{aligned}\widehat{u}_{n+1} &= \widehat{u}_n E_1 + h^{-p} M^{-p-1}[\phi_1 N(\widehat{u}_n, t_n) \\ &+ 2\phi_2(N(a_n, t_n + h/2) + N(b_n, t_n + h/2)) \\ &+ \phi_3 N(c_n, t_n + h)];\end{aligned}$$

with $E_1 = e^{hM}$ *and* $E_2 = e^{hM/2}$.

The following computations are carried out with the number of Fourier modes N_x and N_y, that should be high enough in order to achieve a good precision, and a space computational domain large enough, to ensure periodicity of the solution. Note that the number of Fourier modes depends on the size of the domain, and will increase for the high wave numbers when a blow-up occurs.

A. Numerical experimentations

In order to control the accuracy of the computations, we compute $E(t)$ by the FFT and define

$$\Delta = \left| \frac{E(t)}{E(o)} - 1 \right|. \tag{24}$$

It was reported in [9] that Δ overestimates the numerical precision. This does not evidently make sense if the numerical spatial resolution is not of the same order; i.e. if the Fourier coefficients $\widehat{u}(k_x, k_y)$ do not decrease to the same magnitude, for large numbers k_x and k_y. Therefore we shall use equation (24) and Fourier coefficients as reliable indicators for the accuracy tests.

1- L_2-critical case: in this part, we study the solutions of equation (2) with $\lambda = 1$ for $p = \frac{4}{5}$. This nonlinearity is not very relevant for applications, but it is mathematically interesting. Here we consider the problem with different initial data.
We first study the GKPI-BO using initial data (9) with $\beta = 1$ such that the inital energy is positive. The calculation is performed on $[-5, 5]^2$ with $N_x = Ny = 2^9$ and a time step $\Delta t = 0.0005$. The relative computed energy is conserved up to 10^{-8} after 1000 iterations. From the results shown in Fig.2., there is no ascertainment of a blow-up, and this is even more obvious from the norms shown in Fig.2. (bottom), both $\|u\|_\infty$ and $\|u_y\|_2$ appear to be monotonically decreasing. The situation is not different for initial data with negative energy, i.e. if we set $u_0(x, y) = 12exp(-(x^2 + y^2))$, use the same computation domain and $N_x = 2^{10}, Ny = 2^{10}$ and a smaller time step for numerical stability reason, $\Delta t = 0.00001$. As can be seen in Fig.3., $\|u\|_\infty$ decreases monotonically and after a some time it increases then decreases, whereas the $\|u_y\|_2$ appears to increase without showing any blow-up and the relative computed energy reached 10^{-6} after 10000 iterations. Note that in this case even the corresponding Fourier coefficients tend to increase (see Fig.3. top right).

2- L_2-supercritical case: we seek solutions of (2) with $\lambda = 1$ considering two cases:
case 1: we take $p = 1$ with positive energy. More exactly, with the initial data $u_0(x, y) = 3exp(-(x^2 + y^2))$, The calculation is performed with $[-20, 20] \times [-5, 5]$, $N_x = Ny = 2^{10}$ and $\Delta t = 0.0001$. The relative computed energy is conserved up to 10^{-11} and in this situation there is no blow-up (see Fig.4.). The norms for this solution shown in Fig.4. (bottom) indicate that $\|u\|_\infty$ decreases monotonically and after a some time it increases then starts to decrease again, whereas $\|u_y\|_2$ appears to increase. these results are qualitatively the same as the ones for the critical case (Fig.3. bottom).
However if we take $u_0(x, y) = 12exp(-(x^2 + y^2))$ i.e. subject to a negative energy, on $[-5, 5]^2$ with $N_x = 2^{12}$, $Ny = 2^{10}$ and a very small timestep $\Delta t = 0.000001$, we get a blow-up (see Fig.5.). The relative computed energy reaches a value arround 10^{-2}.
case 2: for $p = 2$ and initial data (9) with $\beta = 1$, $N_x = Ny = 2^{10}$, $h = 0.0001$, $L_x = 10$, $L_y = 4$, after 1000 iterations, we get a Δ of an order better than 10^{-9}, i.e. there is no blow-up, as can be seen in Fig.6. that the initial hump has been completely radiated away.
The situation is completely different if $\beta = 6$, when the initial energy becomes negative. The calculation is performed for $L_x = L_y = 5$, $N_x = 2^1 1$, $\mathrm{N}_y = 2^1 2$ with 5000 iterations. As can be seen in Fig.7., that the initial minimum appears to blow-up in a point after getting more and more peaks, the code breaks down when $\Delta \simeq 10^{-3}$.
We have to point out that the numerical experimentations were explored for both $\lambda = 1$ and $\lambda = -1$. Here we present the results for $\lambda = 1$ (see Fig.2. - Fig.7.) and $\lambda = -1$ (see Fig.8. - Fig.11.). Note that the obtained results are qualitatively similar for both $\lambda = 1$ and $\lambda = -1$.

VI. Conclusion

In this work, we studied the GKP-BO equations's solutions for $p = \frac{4}{5}$, $p = 1$ and $p = 2$. The numerical results are resumed in the figures Fig.2. - Fig.7., for $\lambda = 1$ and Fig.8. - Fig.11. for $\lambda = -1$, where we plot the solution, its corresponding Fourier coefficients, $\|u\|_\infty$ and $\|u_y\|_2$ to visualise the blowing up behavior according to each case. We remarque that the two cases $\lambda = 1$ and $\lambda = -1$ lead to similar qualitative results but with a slight difference in the plotted curves and conclude that:
1- If $p = \frac{4}{5}$, no blow-up occurs. This is shown in Fig.2. and Fig.3. for $\lambda = 1$ and in Fig. 8. and Fig.9. for $\lambda = -1$ and by $\|u\|_\infty$ which increases monotonically and after a some time it increases.
2- For $p = 1$ and $p = 2$, if we take initial data with positive energy, we get almost the same situation as for the critical case (see Fig.4.& Fig.5. for $\lambda = 1$ and Fig.10. for $\lambda = -1$). However for a negative initial energy we can exhibit a blow-up and this can be seen in Fig.6. and Fig.7. for $\lambda = 1$ and in Fig.11. for $\lambda = -1$.

Hence the blow-up phenomenon's behaviour depends on both an initial data satisfying the constraint (8) and the energy's sign (> 0 or < 0), and this is quite relevant so that when the energy is positive we get no blow-up, whereas for the negative case a blow-up occurs.

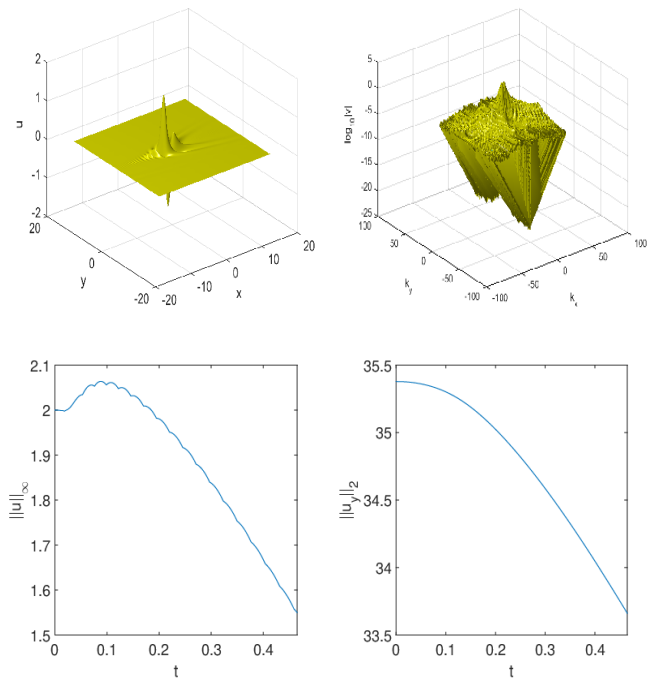

Fig. 2. From top to bottom and left to right, the solution, its Fourier coefficients, $\|u\|_\infty$ and $\|u_y\|_2$ for (1), $\lambda = 1$ with $p = \frac{4}{5}$ and $u_0(x, y) = exp(-(x^2 + y^2))$.

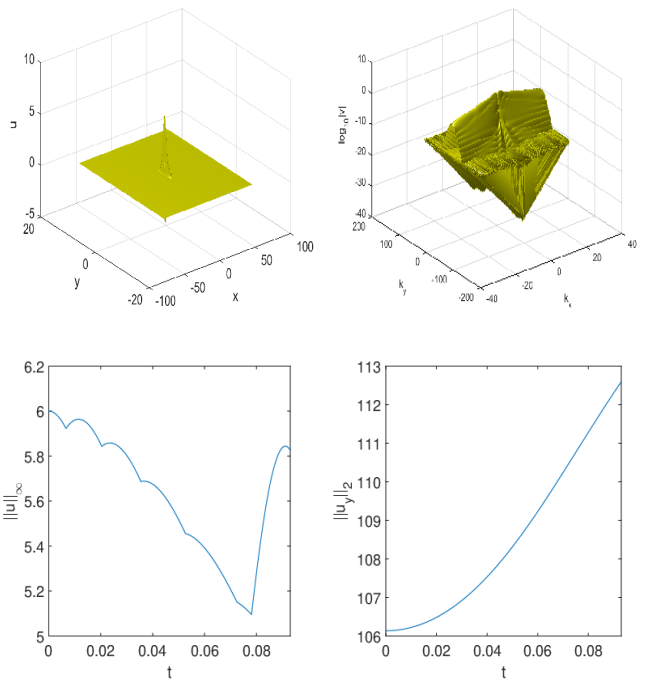

Fig. 4. From top to bottom and left to right, the solution, its Fourier coefficients, $\|u\|_\infty$ and $\|u_y\|_2$ for (1), $\lambda = 1$ with $p = 1$ and $u_0(x, y) = 3exp(-(x^2 + y^2))$.

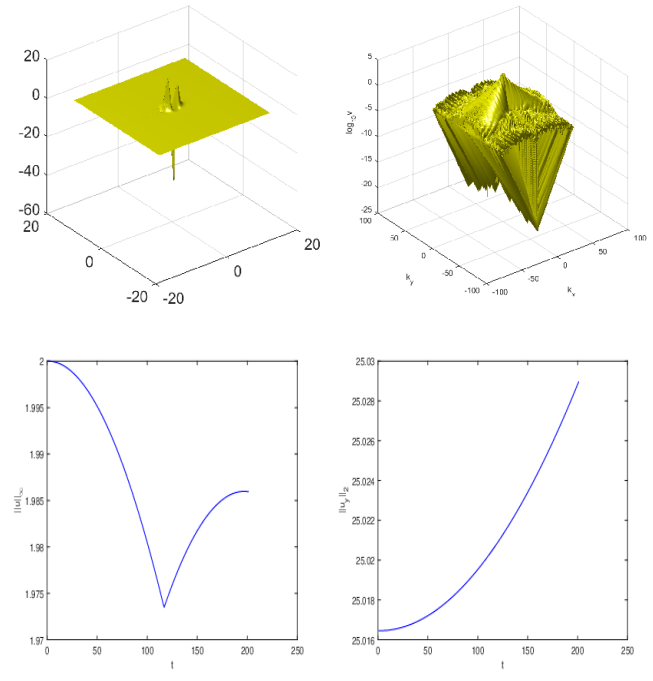

Fig. 3. From top to bottom and left to right, the solution, its Fourier coefficients, $\|u\|_\infty$ and $\|u_y\|_2$ for (1), $\lambda = 1$ with $p = \frac{4}{5}$ and $u_0(x, y) = 12exp(-(x^2 + y^2))$.

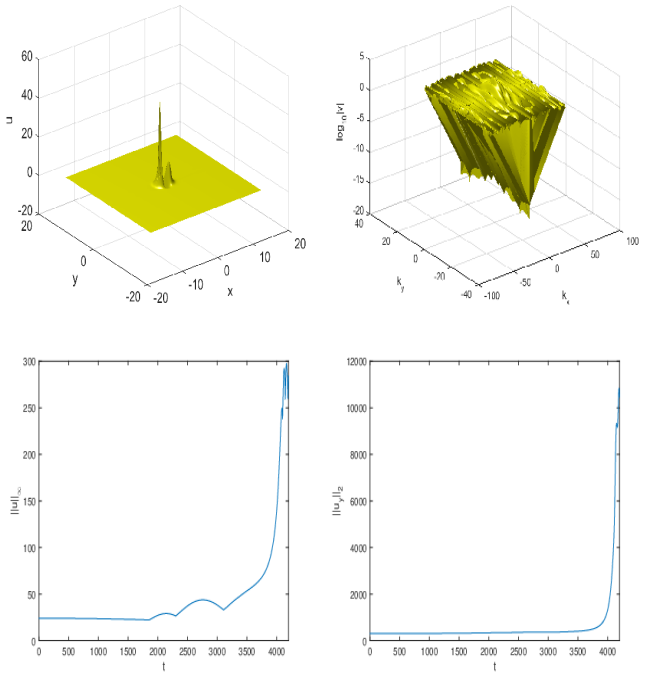

Fig. 5. From top to bottom and left to right, the solution, its Fourier coefficients, $\|u\|_\infty$ and $\|u_y\|_2$ for (1), $\lambda = 1$ with $p = 1$ and $u_0(x, y) = 12exp(-(x^2 + y^2))$.

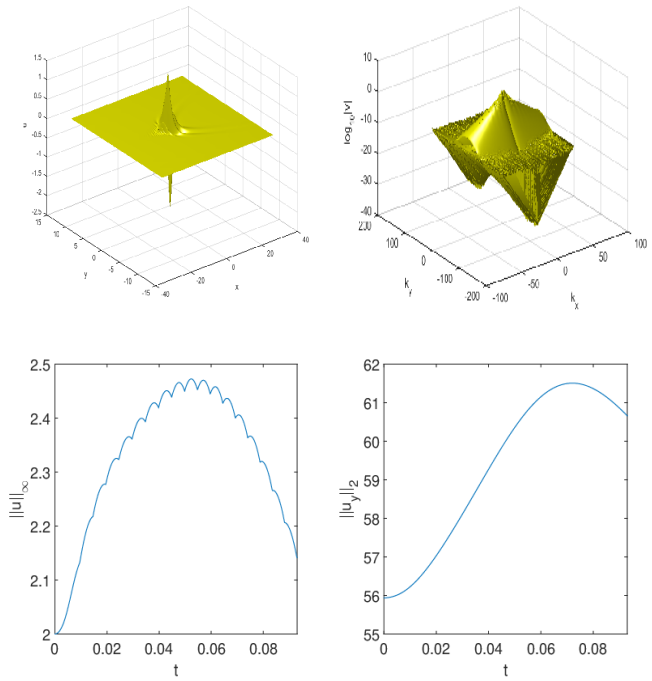

Fig. 6. From top to bottom and left to right, the solution, its Fourier coefficients, $\|u\|_\infty$ and $\|u_y\|_2$ for (1), $\lambda = 1$ with $p = 2$ and $u_0(x, y) = exp(-(x^2 + y^2))$.

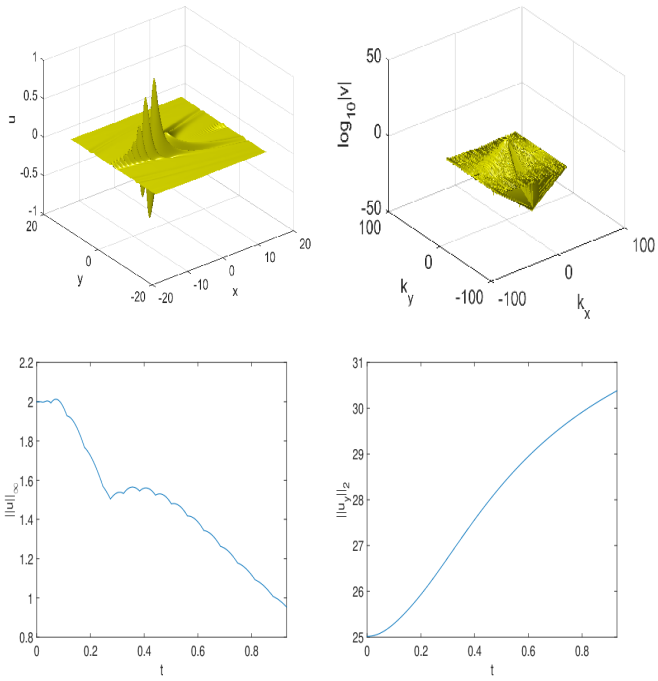

Fig. 8. From top to bottom and left to right, the solution, its Fourier coefficients, $\|u\|_\infty$ and $\|u_y\|_2$ for (1), $\lambda = -1$ with $p = \frac{4}{5}$ and $u_0(x, y) = exp(-(x^2 + y^2))$.

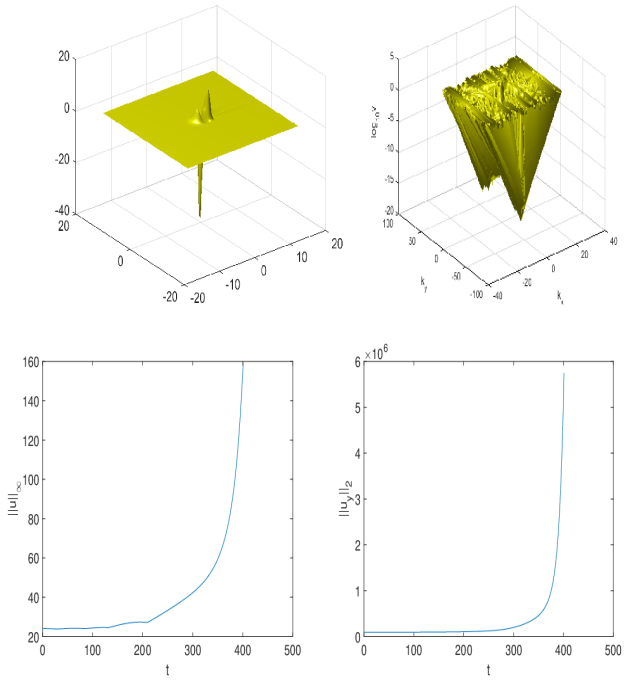

Fig. 7. From top to bottom and left to right, the solution, its Fourier coefficients, $\|u\|_\infty$ and $\|u_y\|_2$ for (1), $\lambda = -1$ with $p = 2$ and $u_0(x, y) = 6exp(-(x^2 + y^2))$.

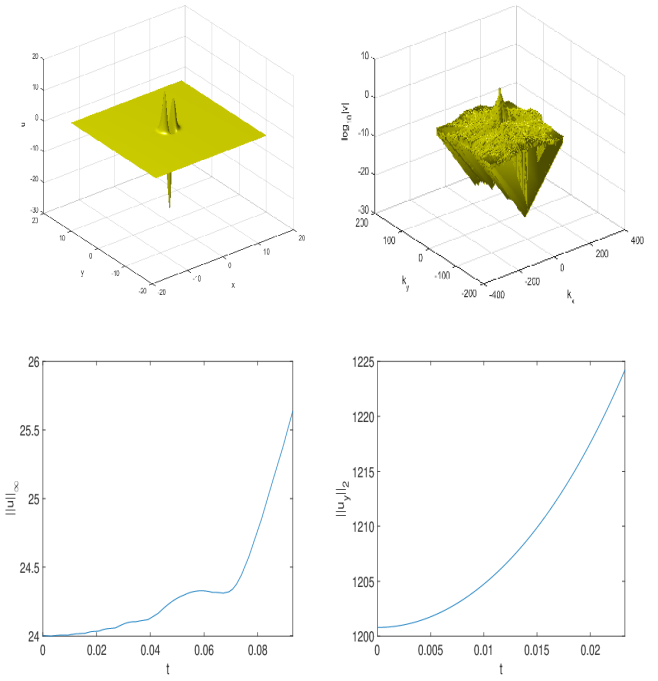

Fig. 9. From top to bottom and left to right, the solution, its Fourier coefficients, $\|u\|_\infty$ and $\|u_y\|_2$ for (1), $\lambda = -1$ with $p = \frac{4}{5}$ and $u_0(x, y) = 12exp(-(x^2 + y^2))$.

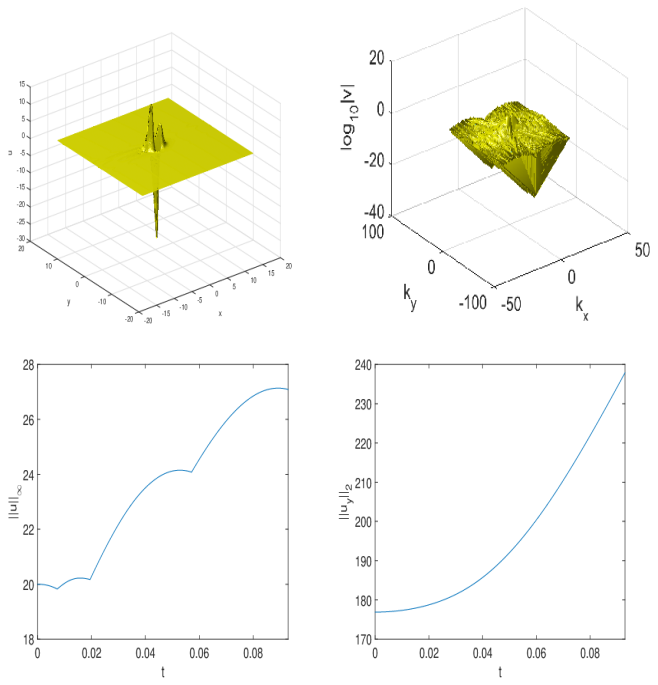

Fig. 10. From top to bottom and left to right, the solution, its Fourier coefficients, $\|u\|_\infty$ and $\|u_y\|_2$ for (1), $\lambda = -1$ with $p = 1$ and $u_0(x, y) = 3exp(-(x^2 + y^2))$.

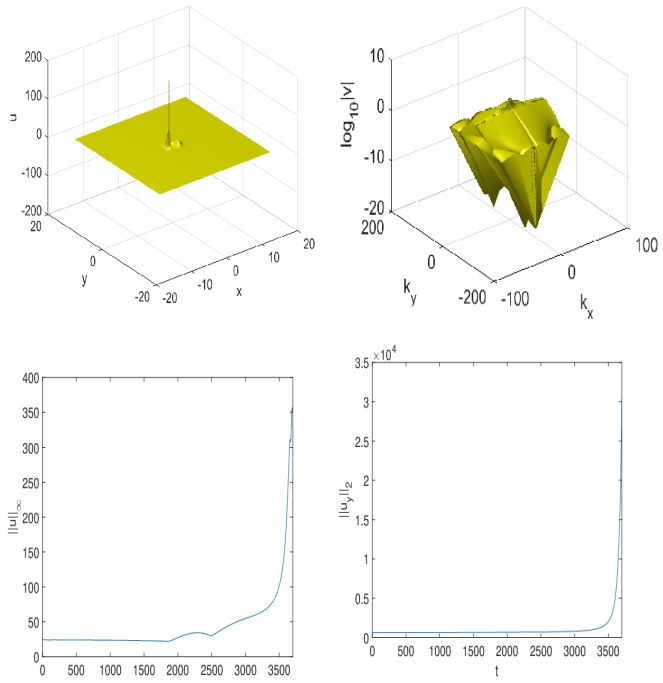

Fig. 11. From top to bottom and left to right, the solution, its Fourier coefficients, $\|u\|_\infty$ and $\|u_y\|_2$ for (1), $\lambda = -1$ with $p = 1$ and $u_0(x, y) = 12exp(-(x^2 + y^2))$.

REFERENCES

[1] C. Canuto, M. Y. Hussaini, A. Quarteroni, and T. A. Zang, *Spectral Methods in Fluid Dynamics*, Vol. 1, Springer (2006)

[2] A. Esfahani, *Remarks on solitary waves of the generalized two dimensional Benjaminâ"Ono equation*,Applied Mathematics and Computation 218 (2011) 308–323

[3] B. Gou, Y. Han, *Remarks on the generalized Kadomtsevâ"Petviashvili equations and two-dimensional Benjaminâ"Ono equations*, Proc. Royal Soc. London Sec. A 452 (1996) 1585–1595

[4] B. Harrop-Griffiths and J.L. Marzuola, *Small data global solutions of the Camassa- Choi equation*, Nonlinearity 31 (2018), 1868–1904

[5] K.R. Helfrich and W.K. Melville, *Long nonlinear internal waves*, Ann. Rev. Fluid Mech 38 (2006), 395–425

[6] A.-K. Kassam and L. N. Trefethen, *Fourth order time-stepping for stiff pdes*, SIAM J. Sci. Comput 26 (2005), 1214–1233

[7] Kato, T.*Quasi-linear equations of evolution, with applications to partial differential equations*. Springer Lecture Notes in Mathematics 448 (1975), 25–70

[8] C. Klein and R. Peter, *Numerical study of blow-up in solutions to generalized Kadomtsev-Petviashvili equations*, Discrete Continuous Dynamical Systems - B, 19(6): 1689-1717. doi: 10.3934/dcdsb.2014.19.1689

[9] C. Klein and K. Roidot, *Fourth order time-stepping for Kadomtsev-Petviashvili and Davey-Stewardson equations*, SIAM J. Sci. Comput. 33 (2011), 3333–3356

[10] C. Klein, C. Sparber, and P. Markowich, *Numerical study of oscillatory regimes in the Kadomtsev- Petviashvili equation*, J. Nonl. Sci. 17 (2007), 429–470.

[11] F. Linares, D. Pilod and J.-C. Saut, *The Cauchy problem for the fractional Kadomtsev- Petviashvili equations*, SIAM J. Math. Anal. 50 (3) (2018), 3172–3209.

[12] Yan Liu, Mingbin WANG, and Lei MENG, *Spectral Collocation Method in the Large Deformation Analysis of Flexible Beam*, IAENG International Journal of Applied Maths, vol. 48, no.4 (2018), 416-423.

[13] F.Z Nouri, D. Sloan,*A Comparison of Fourier Pseudospectral Methods for the Solution of the Korteweg-de Vries Equation*,J. of Comp. Physics. Vol 83 Issue 2 (1989), 324-344.

[14] G. C. Nwachukwu, and N.E. Mokwunyei, *Generalized Adams-Type Second Derivative Methods for Stiff Systems of ODEs*, IAENG International Journal of Applied Maths, vol. 48, no.4 (2018), 455-465.

[15] J. C. Saut, *Benjamin-Ono and intermediate long wave equations: modeling, IST and PDE* , Preprint (2018)

[16] G. Preciado. López and F. H. Soriano Méndez, *On the existence and analycity of solitary waves solutions to a two-dimesional Benjamin-Ono equation*, preprint (2018)